

This is a repository copy of *Lifetime measurement of the 260 g.s. At SAMURAI*.

White Rose Research Online URL for this paper:

<https://eprints.whiterose.ac.uk/194216/>

Version: Published Version

---

**Article:**

Storck, S., Caesar, C., Kahlbow, J. et al. (58 more authors) (2020) Lifetime measurement of the 260 g.s. At SAMURAI. *Journal of Physics: Conference Series*. 012106. ISSN 1742-6596

<https://doi.org/10.1088/1742-6596/1643/1/012106>

---

**Reuse**

This article is distributed under the terms of the Creative Commons Attribution (CC BY) licence. This licence allows you to distribute, remix, tweak, and build upon the work, even commercially, as long as you credit the authors for the original work. More information and the full terms of the licence here:

<https://creativecommons.org/licenses/>

**Takedown**

If you consider content in White Rose Research Online to be in breach of UK law, please notify us by emailing [eprints@whiterose.ac.uk](mailto:eprints@whiterose.ac.uk) including the URL of the record and the reason for the withdrawal request.

PAPER • OPEN ACCESS

## Lifetime measurement of the $^{26}\text{O}$ g.s. at SAMURAI

To cite this article: S Storck *et al* 2020 *J. Phys.: Conf. Ser.* **1643** 012106

View the [article online](#) for updates and enhancements.

You may also like

- [THE EFFECTS OF THERMONUCLEAR REACTION RATE VARIATIONS ON  \$^{26}\text{Al}\$  PRODUCTION IN MASSIVE STARS: A SENSITIVITY STUDY](#)

Christian Iliadis, Art Champagne, Alessandro Chieffi et al.

- [Solid-State Nanocomposite Electrochromic Pseudocapacitors](#)

Se-Hee Lee, C. Edwin Tracy, Yanfa Yan et al.

- [Halo nuclei, stepping stones across the drip-lines](#)

H Simon



The Electrochemical Society  
Advancing solid state & electrochemical science & technology

243rd ECS Meeting with SOFC-XVIII

Boston, MA • May 28 – June 2, 2023

**Abstract Submission Extended  
Deadline: December 16**

[Learn more and submit!](#)

## Lifetime measurement of the $^{26}\text{O}$ g.s. at SAMURAI

S Storck<sup>1,2</sup>, C Caesar<sup>3,2</sup>, J Kahlbow<sup>1,2</sup>, V Panin<sup>2</sup>, D S Ahn<sup>2</sup>, L Atar<sup>1,2</sup>, T Aumann<sup>1,3</sup>, H Baba<sup>2</sup>, K Boretzky<sup>3,2</sup>, H Chae<sup>4</sup>, N Chiga<sup>2</sup>, S Choi<sup>4</sup>, M L Cortés<sup>2</sup>, D Cortina-Gil<sup>5</sup>, Q Deshayes<sup>6</sup>, P Doornenbal<sup>2</sup>, Z Elekes<sup>7</sup>, N Fukuda<sup>2</sup>, I Gašparić<sup>8,2</sup>, K I Hahn<sup>9</sup>, Z Halász<sup>7</sup>, A Hirayama<sup>11</sup>, J Hwang<sup>4</sup>, N Inabe<sup>2</sup>, T Isobe<sup>2</sup>, S Kim<sup>4</sup>, T Kobayashi<sup>10,2</sup>, D Körper<sup>3</sup>, Y Kondo<sup>11,2</sup>, Y Kubota<sup>2</sup>, I Kuti<sup>7</sup>, C Lehr<sup>1,2</sup>, S Lindberg<sup>12,2</sup>, M Marques<sup>6</sup>, M Matsumoto<sup>11</sup>, T Murakami<sup>13,2</sup>, I Murray<sup>2</sup>, T Nakamura<sup>11,2</sup>, T Nilsson<sup>12</sup>, H Otsu<sup>2</sup>, S Paschalis<sup>14,1</sup>, M Parlog<sup>6</sup>, M Petri<sup>14,1</sup>, D Rossi<sup>1</sup>, A Saito<sup>11</sup>, M Sasano<sup>2</sup>, H Scheit<sup>1</sup>, P Schrock<sup>15</sup>, Y Shimizu<sup>2</sup>, H Simon<sup>3</sup>, D Sohler<sup>7</sup>, O Sorlin<sup>15</sup>, L Stuhl<sup>16</sup>, H Suzuki<sup>2</sup>, I Syndikus<sup>1</sup>, H Takeda<sup>2</sup>, H Törnqvist<sup>1,2,3</sup>, Y Togano<sup>11,2</sup>, T Tomai<sup>11</sup>, T Uesaka<sup>2</sup>, H Yamada<sup>11</sup>, Z Yang<sup>2</sup>, M Yasuda<sup>11</sup>, K I Yoneda<sup>2</sup> for the SAMURAI20 Collaboration

<sup>1</sup>Institut für Kernphysik, TU Darmstadt

<sup>2</sup>RIKEN Nishina Center

<sup>3</sup>GANIL Helmholtzzentrum für Schwerionenforschung, Darmstadt

<sup>4</sup>Department of Physics, Seoul National University

<sup>5</sup>Departamento de Física de Partículas, Universidade de Santiago de Compostela

<sup>6</sup>LPC, Caen

<sup>7</sup>ATOMKI, Debrecen

<sup>8</sup>Ruder Bošković Institute, Zagreb

<sup>9</sup>Department of Physics, Ewha Womens University

<sup>10</sup>Department of Physics, Tohoku University

<sup>11</sup>Department of Physics, Tokyo Institute of Technology

<sup>12</sup>Department of Physics, Chalmers University of Technology

<sup>13</sup>Department of Physics, Kyoto University

<sup>14</sup>Department of Physics, University of York

<sup>15</sup>GANIL, Caen

<sup>16</sup>Center for Nuclear Studies (CNS), University of Tokyo

E-mail: sstorck@ikp.tu-darmstadt.de

**Abstract.** The ground state of the neutron unbound nucleus  $^{26}\text{O}$  is speculated to have a lifetime in the pico-second regime. In order to determine the decay lifetime of the  $^{26}\text{O}$  ground state with high sensitivity and precision, a new method has been applied. The experiment was performed in December 2016 at the Superconducting Analyzer for Multi-particle from Radio Isotope Beams (SAMURAI) at the Radioactive Isotope Beam Factory (RIBF) at RIKEN. A  $^{27}\text{F}$  beam was produced in the fragment separator BigRIPS and impinged on a W/Pt target stack where  $^{26}\text{O}$  was produced. According to the lifetime, the decay of  $^{26}\text{O}$  happens either in or outside the target. Thus, the velocity difference between the decay neutrons and the fragment  $^{24}\text{O}$  delivers a characteristic spectrum from which the lifetime can be extracted.



## 1. Introduction

The neutron drip line, from where on nuclei are not longer bound, is experimentally established only up to oxygen ( $Z = 8$ ). Theoretical predictions of the location of the neutron drip line are very difficult since the interaction of nucleons for large neutron to proton asymmetries is not well known. The behavior of the drip line around  $Z = 8$  is exceptional. From oxygen to fluorine a sudden change of stability happens; by “adding” one proton, at least six more neutrons can be bound. This is often referred to as the “oxygen anomaly”. Modern ab-initio theories aim to calculate the nuclear structure in a systematic way. In interactions determined e.g. from chiral EFT three-nucleon forces emerge naturally. In such a framework, for instance Otsuka *et al.* show the importance of  $3N$  interactions to describe the oxygen chain leading to  $^{24}\text{O}$  being the last bound oxygen isotope [1]. The magic number  $N = 20$  that applies for stable nuclei is quenched for neutron-rich nuclei as the island of inversion shows. Exploring nuclei beyond the oxygen drip line is important to understand this behavior.

The lifetimes of proton-rich nuclei beyond the drip line can still be rather long ( $\sim$  ms) due to the Coulomb barrier [2]. Neutron-rich nuclei beyond the neutron drip line usually decay very fast due to the missing Coulomb barrier. Typical lifetimes for neutron unbound states are in the order of  $< 10^{-18}$  s [3]. Theory calculations predict that  $^{26}\text{O}$  is a promising candidate for radioactive decay via neutron emission with a lifetime in the pico-second regime [4]. It is only unbound by  $18 \pm 3(\text{stat}) \pm 4(\text{syst})$  keV [5]. The decay could therefore be hindered by the centrifugal barrier with the two valence neutrons being in the  $d_{3/2}$  shell increasing the lifetime. The level scheme of  $^{26}\text{O}$  is shown in Fig. 1 as found by Kondo *et al.* [5]. The sequential decay via the ground state of  $^{25}\text{O}$  is energetically forbidden, which makes  $^{26}\text{O}$  a true two-neutron emitter.

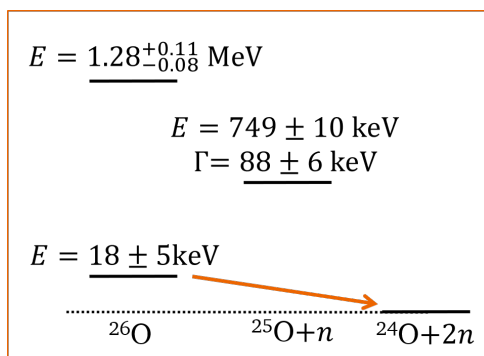


Figure 1: Level scheme of  $^{26}\text{O}$  following [5]. The decay of the  $2n$  emitter  $^{26}\text{O}$  g.s. is only  $18 \pm 5$  keV.

At the National Superconducting Cyclotron Laboratory (NSCL) at the Michigan State University (MSU) the half-life of  $^{26}\text{O}$  was determined to be  $T_{1/2} = 4.5^{+1.1}_{-1.5}(\text{stat}) \pm 3(\text{syst})\text{ps}$ , which corresponds to a lifetime of  $\tau = 6.5$  ps [6]. In this measurement,  $^{26}\text{O}$  was produced from proton removal from a  $^{27}\text{F}$  beam with 82 MeV/u on a  $705 \text{ mg/cm}^2$   $^9\text{Be}$  reaction target. The two neutrons are measured by the Modular Neutron Array (MoNA) in coincidence with the fragment. The width of the resonance is expected to be too small to be measured directly with achievable energy resolutions, which makes a different approach necessary [4]. The lifetime was extracted from a shift in the mean velocity-difference of neutrons and the fragment. However, this method depends on the precise calibration of both velocities, which gives rise to the large systematic uncertainty.

## 2. Measurement Method

Recently, a new method was developed by Kahlbow *et al.* to measure the lifetime  $\tau$  of a nucleus that decays via neutron emission [3]. The measurement principle was used in this experiment to determine the lifetime of  $^{26}\text{O}$ .

$^{26}\text{O}$ , with a lifetime  $\tau$ , is produced via proton removal from  $^{27}\text{F}$  and will then decay into  $^{24}\text{O}$  and two neutrons. The decay will occur inside or outside of the target material, producing different shapes in the velocity-difference distribution  $\Delta\nu$  between the decay neutrons and the residual nucleus. Prompt decays in the target will give rise to a “box”-like shape in the spectrum, whereas delayed decays will produce a sharp peak as shown in Fig. 2. The characteristic shape of the velocity-difference distribution can be analyzed to determine the lifetime, where an absolute calibration of  $\Delta\nu$  is not necessary.

The target material ( $Z, \rho$ ) has to be chosen such that on the one hand the stopping power of the target is maximized to be able to see a difference in the velocities of the fragment and neutrons, and on the other hand that a sufficient number of decays will happen outside of the target. The material will continuously slow down the fragments in the material, and this causes the broad shape in the spectrum if the decay happens inside. After the  $^{26}\text{O}$  passed the material, the fragments will not be slowed down any longer creating the sharp peak of outside decays. The width of this peak is dominated by the neutron time-of-flight resolution. Thus, this method is only applicable at setups with a good time-of-flight resolution such as SAMURAI.

The idea is to compare the experimental spectrum with simulated spectra. The simulations will be performed for several lifetimes and then fit to the experimental spectrum. Reference [3] shows a simulation example for  $\tau = 6.5\text{ ps}$ , depicted in Fig. 2. From the unnormalized  $\chi^2$  distribution, the lifetime can be extracted (smallest  $\chi^2$ ), see Fig. 3. The determined lifetime from the  $\chi^2$  was  $\tau = 6.49 \pm 0.08\text{ ps}$  [3].

In order to be sensitive to a range of lifetimes, a stack of targets is proposed to be used in [3]. The sensitivity to a certain lifetime depends on the combination of the incoming energy and the target thickness. The individual target sheets decrease in thickness with beam direction. Short lifetimes are measured with low energies and thin targets to make sure that a sufficient amount of decays occur both inside and outside of the target. A simulated velocity-difference spectrum for a setup with eight Pt target sheets and  $^{27}\text{F}$  beam of  $200\text{ MeV/u}$  is shown in Fig. 4. One can see that the peak and “box” structure repeats for every target foil. Additionally, the ratio of outside to inside decays increases and the energy of the particle decreases from target to target. The new method presented above is predicted by Monte Carlo simulations to measure lifetimes down to  $0.2\text{ ps}$  within  $5\sigma$  using eight targets [3].

### 3. Experimental Setup

The experiment was performed at the Rare Isotope Beam Facility (RIBF) at RIKEN in Japan at the SAMURAI-setup. At RIBF very high intensities of neutron-rich beams can be reached. The secondary beams,  $^{27}\text{F}$ ,  $^{26}\text{F}$ , and  $^{24}\text{O}$ , were provided by the RIKEN Projectile Fragment Separator (BigRIPS) and produced from  $^{48}\text{Ca}$  primary beam. The reactions took place at the SAMURAI experimental setup [7]. The experiment was performed in inverse kinematics at relativistic energies. The detector setup allows the performance of kinematically complete measurements where the momenta of all particles are measured, including those of the neutrons, with large acceptance.

The experiment was dedicated to explore a new method and study the neutron-radioactive decays of the candidate nucleus  $^{26}\text{O}$ , which is produced from proton removal on  $^{27}\text{F}$  with  $220\text{ MeV/u}$ . It is necessary to measure the incoming  $^{27}\text{F}$ , the outgoing  $^{24}\text{O}$ , and the two neutrons in coincidence. The experiment was part of the NeuLAND at SAMURAI-campaign where the  $\text{R}^3\text{B}$  neutron detector NeuLAND-demonstrator (New Large Area Neutron Detector) [8] was combined with NEBULA (Neutron Detection System for Breakup of Unstable Nuclei with Large Acceptance) to increase the multi-neutron detection efficiency.

The experimental setup is shown in Fig. 6. For the reaction target, tungsten and platinum were chosen as target materials because of their large  $Z$  (74 and 78) and high mass density of  $19.25\text{ g/cm}^3$  and  $21.45\text{ g/cm}^3$ , respectively. The reaction target consisted of six individual target

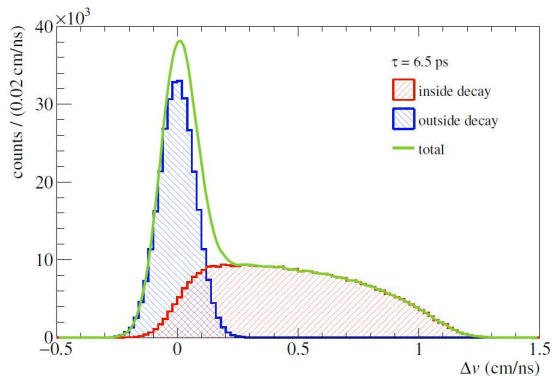


Figure 2: Simulated velocity-difference spectrum for a lifetime of 6.5 ps with one Pt target. The decays inside the target produce a “box”-like shape in the spectrum (red), whereas the delayed decays after the target lead to a sharp peak (blue). The total distribution is given by the green line. The plot is taken from [3].

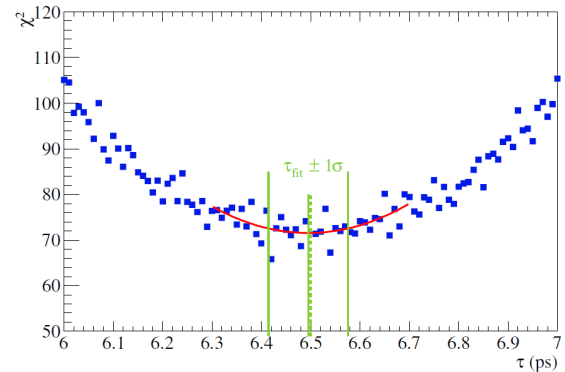


Figure 3: The pseudo-experimental spectrum is fit to simulated spectra for different lifetimes. In order to get the lifetime,  $\chi^2$  of each fit is shown over the simulated lifetime and fit with a polynomial of the second order. The minimum of the fit gives the lifetime. For the example in Fig. 2, the deduced lifetime with this method is  $\tau = 6.49 \pm 0.08$  ps. The plot is taken from [3].

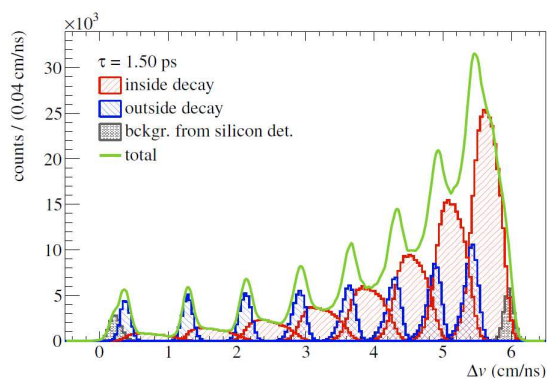


Figure 4: Simulated velocity-difference spectrum for a lifetime of 1.5 ps with a target stack of eight Pt targets. The structure of the target stack is visible in the spectrum. The peak with the largest velocity difference belongs to the first target. The ratio of outside to inside decays increases from target to target. By using a stack of targets the precision of the method is increased and a range of lifetimes can be probed [3].

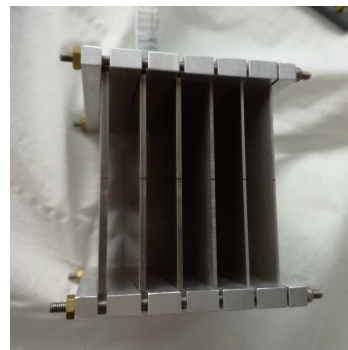


Figure 5: The target used in the experiment is a combination of six individual target sheets. With the beam coming from the left, the first four are made of tungsten and the last two are made of platinum. The thickness decreases with beam direction.

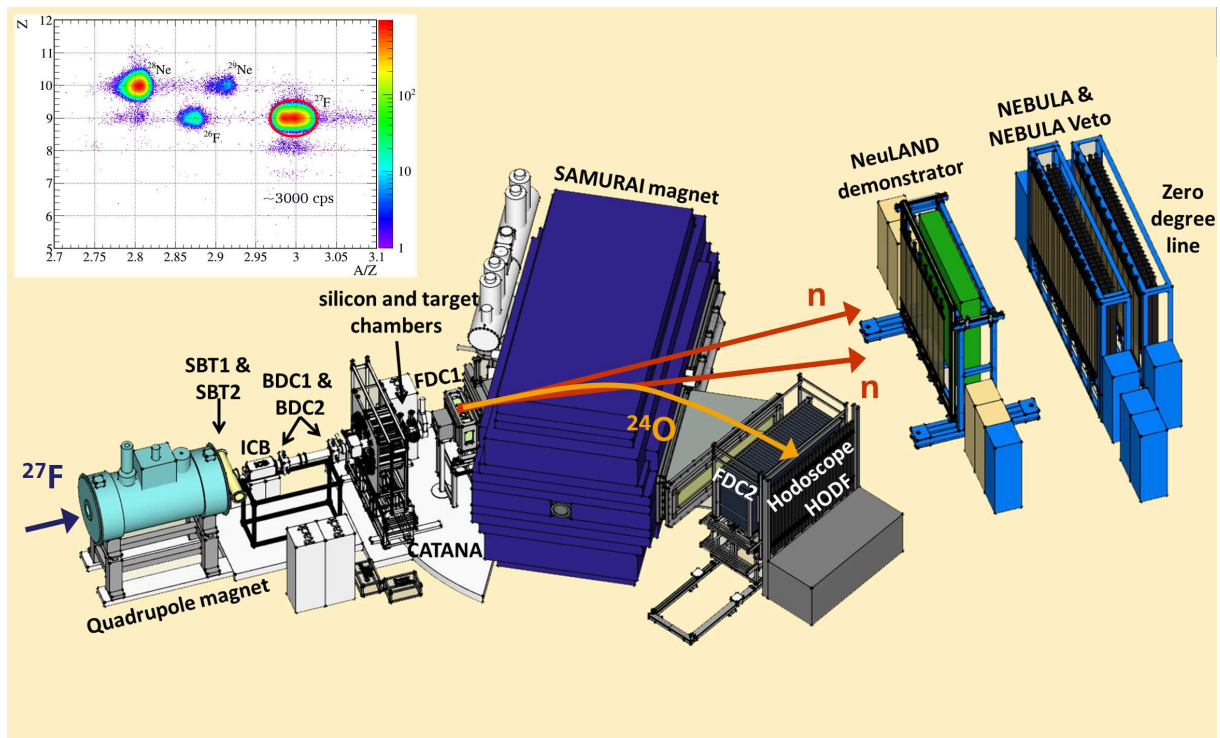


Figure 6: Setup of the experiment. After the last quadrupole magnet of BigRIPS the start detectors SBT 1 and 2 are placed. They are followed by the ICB for energy loss measurement and the two BDCs for tracking. The CATANA  $\gamma$ -detector was not used in the experiment. The target is placed between silicon detectors in the two target chambers. The FDCs track the charged particles through the SAMURAI magnet which are measured in the Hodoscope. The neutrons are not bent by the magnetic field and are detected by the NeuLAND and NEBULA neutron detectors, which are placed at zero degrees. The incoming particle identification for the  $^{27}\text{F}$  beam with a rate of  $\sim 3000$  cps is shown in the plot.

sheets decreasing in thickness, which were mounted with a space of 8 mm inbetween. The area densities decreased with beam direction from  $3.93 \text{ g/cm}^2$  for the first target to  $1.32 \text{ g/cm}^2$  to the last target.

The incoming beam is identified using the ionization chamber (ICB) and tracked with the drift chambers (BDC 1 & 2). The time-of-flight measurement is initiated by the plastic scintillators SBT 1 & 2. The target was surrounded by three  $300 \mu\text{m}$  thick single-area silicon detectors. Those are necessary to identify the incoming beam particles directly in front of the target and the fragments after the proton removal reaction to select the isotope of interest. One silicon detector was installed in front of the target stack and two behind. The target in which the reaction happened can already be identified in the  $\Delta\nu$ -spectrum, which makes it unnecessary to measure the energy loss between the individual target sheets. The silicon detectors act as targets themselves and therefore contribute to the background as indicated by the gray peaks in Fig. 4. The background originating from the silicon detectors can not easily be determined by an empty target run since the energy loss from the target would be missing and the peaks of the individual silicon detectors would overlap in the  $\Delta\nu$ -spectrum. However, the background contributions can be determined from a reference measurement with the  $^{26}\text{F}$  secondary beam where  $^{25}\text{O}$  is produced from proton removal but no lifetime is expected ( $\tau < 10^{-21} \text{ s}$ ) and thus a flat spectrum. The secondary beam  $^{24}\text{O}$ , with  $210 \text{ MeV/u}$  and a rate of  $\sim 1000$  cps, is very sharp in energy and

necessary for the calibration of the detectors concerning the time-of-flight. After the reaction, charged fragments are deflected by the magnet and tracked with additional drift chambers and finally measured in the Hodoscope, a plastic scintillator wall. The large acceptance that the SAMURAI setup provides is crucial for measuring the fragments. Due to the broad range of energy losses in the target, the fragments cover a large  $B\rho$  region. The experimental data is still under analysis.

### Acknowledgments

We would like to thank the RIKEN Nishina Center accelerator department for providing a stable and high intensity  $^{48}\text{Ca}$  primary beam and the BigRIPS team for their efforts in preparing the secondary beams. This work has been supported by DFG grant no. SFB 1245, BMBF contract 05P15RDFN1 and GSI-TU Darmstadt cooperation agreement.

### References

- [1] Otsuka T, Suzuki T, Holt J D, Schwenk A and Akaishi Y 2010 *Physical Review Letters* **105**(3) 032501 URL <https://link.aps.org/doi/10.1103/PhysRevLett.105.032501>
- [2] Pfützner M 2013 *Physica Scripta* **T152**
- [3] Kahlbow J, Caesar C, Aumann T, Panin V, Paschalis S, Scheit H and Simon H 2017 *Nuclear Instruments and Methods in Physics Research Section A: Accelerators, Spectrometers, Detectors and Associated Equipment* **866** 265–271
- [4] Grigorenko L, Mukha I, and Zhukov M 2013 *Physical Review Letters* **111**
- [5] Kondo Y, Nakamura T, Tanaka R, Minakata R, Ogoshi S, Orr N, Achouri N, Aumann T, Baba H, Delaunay F, Doornenbal P, Fukuda N, Gibelin J, Hwang J, Inabe N, Isobe T, Kameda D, Kanno D, Kim S, Kobayashi N, Kobayashi T, Kubo T, Leblond S, Lee J, Marqués F, Motobayashi T, Murai D, Murakami T, Muto K, Nakashima T, Nakatsuka N, Navin A, Nishi S, Otsu H, Sato H, Satou Y, Shimizu Y, Suzuki H, Takahashi K, Takeda H, Takeuchi S, Togano Y, Tuff A, Vandebrouck M and Yoneda K 2016 *Physical Review Letters* **116** URL <http://dx.doi.org/10.1103/PhysRevLett.116.5493>
- [6] Kohley Z, Baumann T, Bazin D, Christian G, DeYoung P A, Finck J E, Frank N, Jones M, Lunderberg E, Luther B, Mosby S, Nagi T, Smith J K, Snyder J, Spyrou A and Thoennessen M 2013 *Physical Review Letters* **110** URL <http://dx.doi.org/10.1103/PhysRevLett.110.152501>
- [7] Kobayashi T, Chiga N, Isobe T, Kondo Y, Kubo T, Kusaka K, Motobayashi T, Nakamura T, Ohnishi J, Okuno H, Otsu H, Sako T, Sato H, Shimizu Y, Sekiguchi K, Takahashi K, Tanaka R and Yoneda K 2013 *Nuclear Instruments and Methods in Physics Research Section B: Beam Interactions with Materials and Atoms* **317** 294–304
- [8] The  $\text{R}^3\text{B}$  Collaboration 2011 Technical report for the design, construction and commissioning of neuland: The high-resolution neutron time-of-flight spectrometer for  $\text{R}^3\text{B}$  Tech. rep.